**FIGURES**

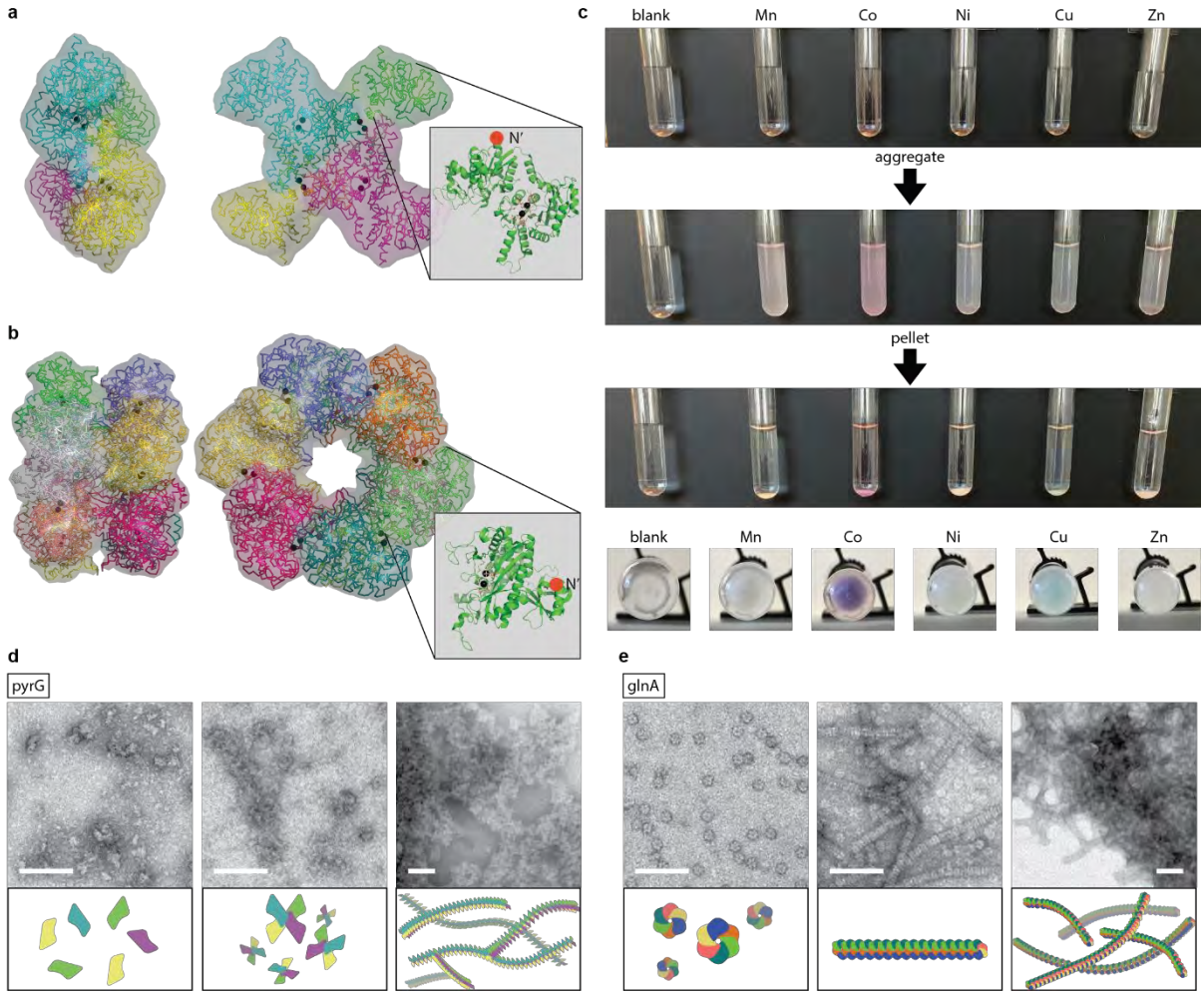


**Figure 1 | Using pyrG and glnA as aggregation agents for heavy metal removal. a**) pyrG representative crystal structure 1S1M is shown, which contains 4 identical monomers shaped into an 'X'. Each monomer contains 2 divalent metal binding pockets. The N'terminus is highlighted to show the region in which metal binding appendages can be attached to further enhance metal binding. **b**) A similar structure is shown for glnA using representative crystal structure 1FPY shaped as two stacked hexagons. Each monomer has two metal binding pockets, and N'terminus is highlighted. **c**) Visual representation of metal binding and aggregation of glnA. Metal and protein concentration were at 10 mM and 500 $\mu$M respectively. **d, e**) HRTEM images of pyrG and glnA, respectively at different levels of aggregation in the presence of Zn. Illustrations below the hypothesized structure and formation of these aggregating chains. Scale bars represent 50 nm.

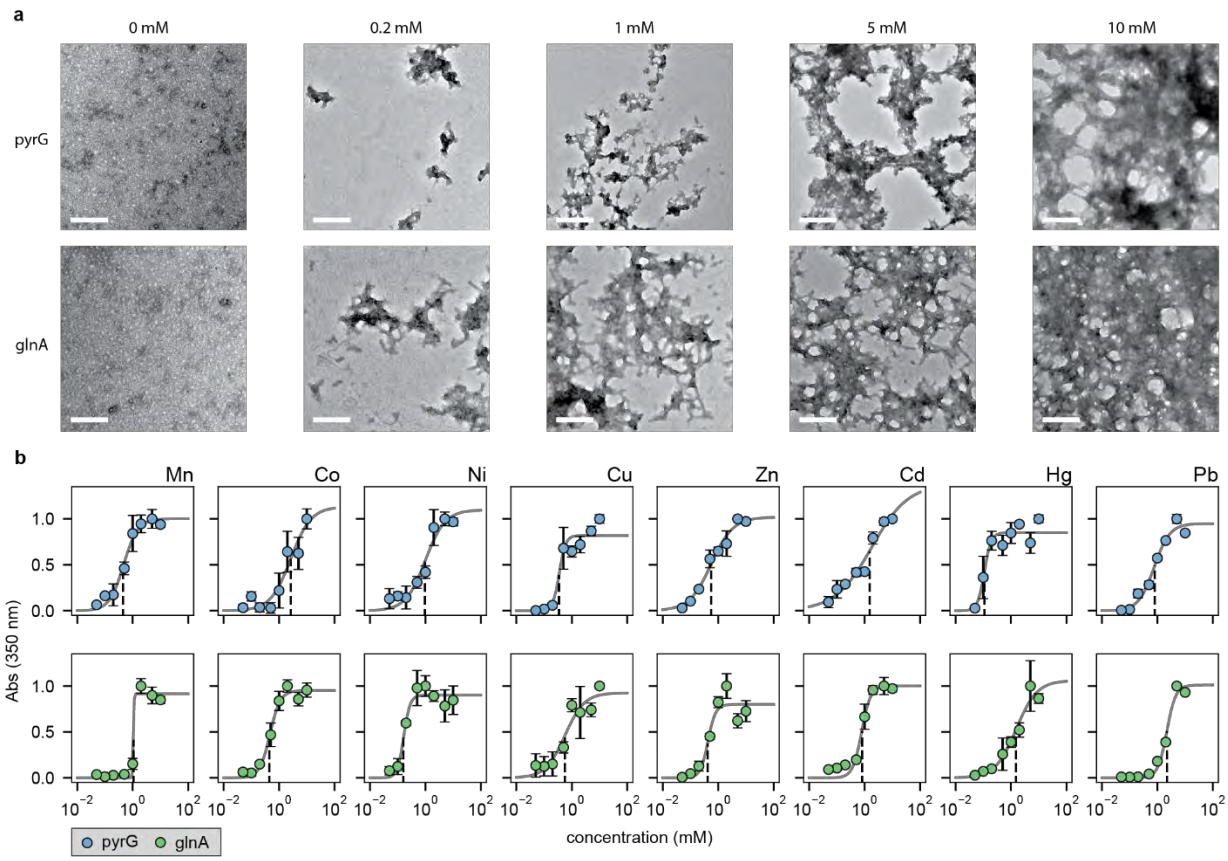


**Figure 2 | Measuring metal induced aggregation responsiveness and intensity for pyrG and glnA. a**) Top/bottom row are pyrG and glnA respectively. Columns represent concentrations of Zn which was used to induce aggregation, with progressively higher concentrations leading to higher levels of aggregation. Scale bars represent 200 nm for all images. **b**) pyrG and glnA were titrated with metals to measure the level of aggregation as a function of metal concentration. Aggregation was quantitatively measured using 350 absorbance readings (Error! Reference source not found.). For all data, the mean ± s.d. of three replicates are shown.

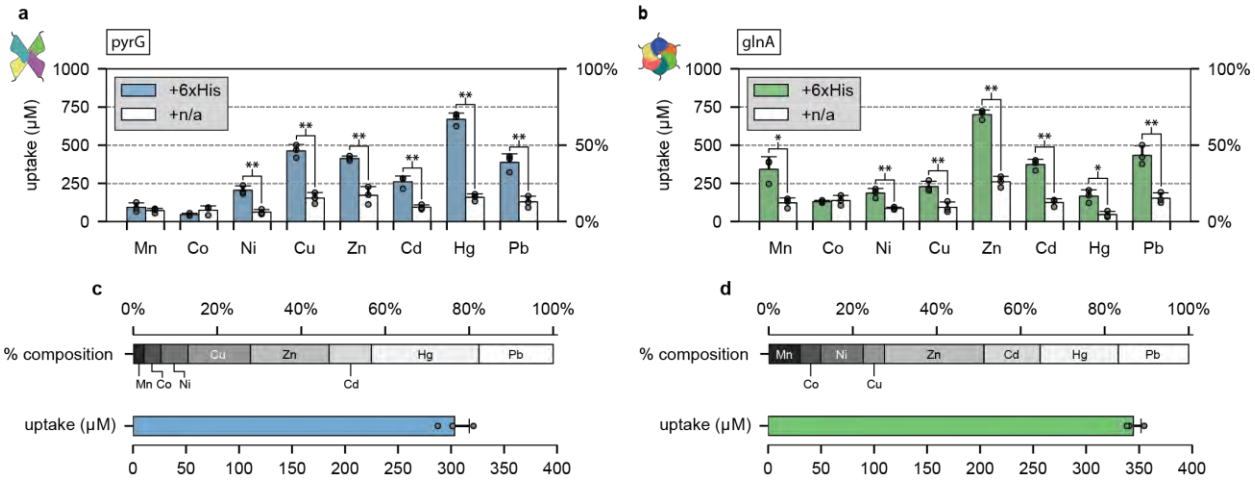


**Figure 3 | Metal removal of Mn, Co, Ni, Cu, Zn, Cd, Hg, and Pb were measured for pyrG and glnA**. **a, b**) Removal of 1 mM metals were individually measured for pyrG or glnA, respectively. Controls (white bars) are pyrG and glnA cleaved of its 6xHis tag fusion and measured for metal uptake. **c, d**) Metal removal of mixtures of the metals specified (totaling 1 mM, or 125 $\mu$M each) were measured for pyrG or glnA, respectively. Top bar represents the percent composition of the metals removed, whereas the bottom bar represents the total amount of metal removed. For all data, the mean $\pm$ s.d. of three replicates are shown.

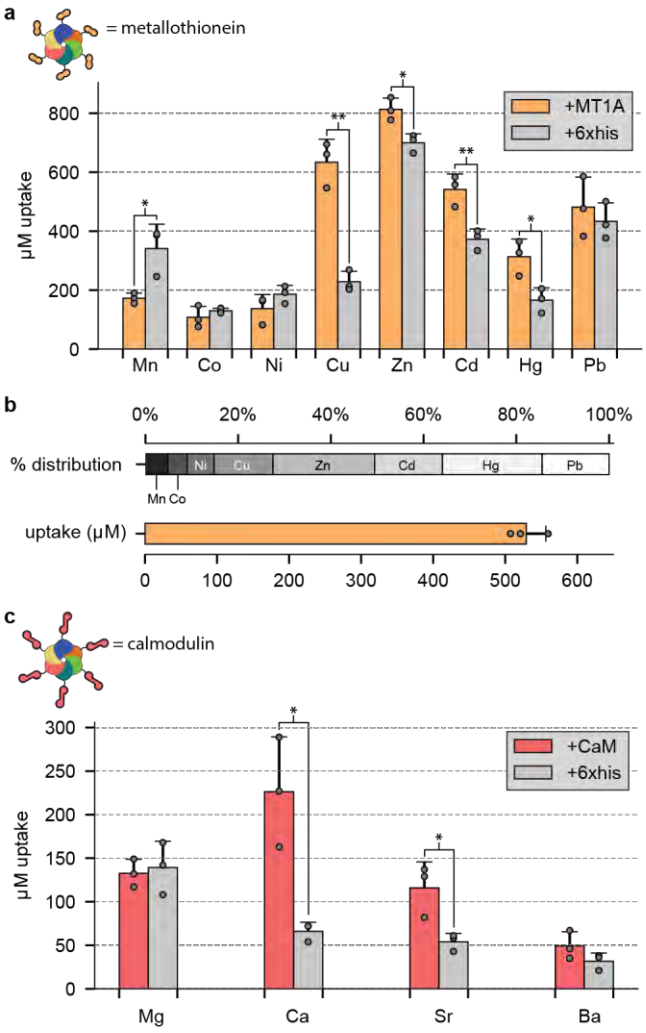


**Figure 4 | Substituting the 6xHis tag with plant MT1A or yeast calmodulin alters metal binding preference and metal removal capability. a**) The same metal removal experiment was performed for +MT1 as was with glnA with a 6xHis tag. Individual metal preference skews more towards copper, zinc, cadmium, and mercury ($p < .05$). **b**) Likewise, the same metal mixture removal experiment was performed, where the top bar represents the percent composition of removed metals, and the bottom bar represents total metal removed. **c**) +CaM were aggregated with Zn and tested for Mg, Ca, Sr, and Ba removal. For all data, the mean $\pm$ s.d. of three replicates are shown.

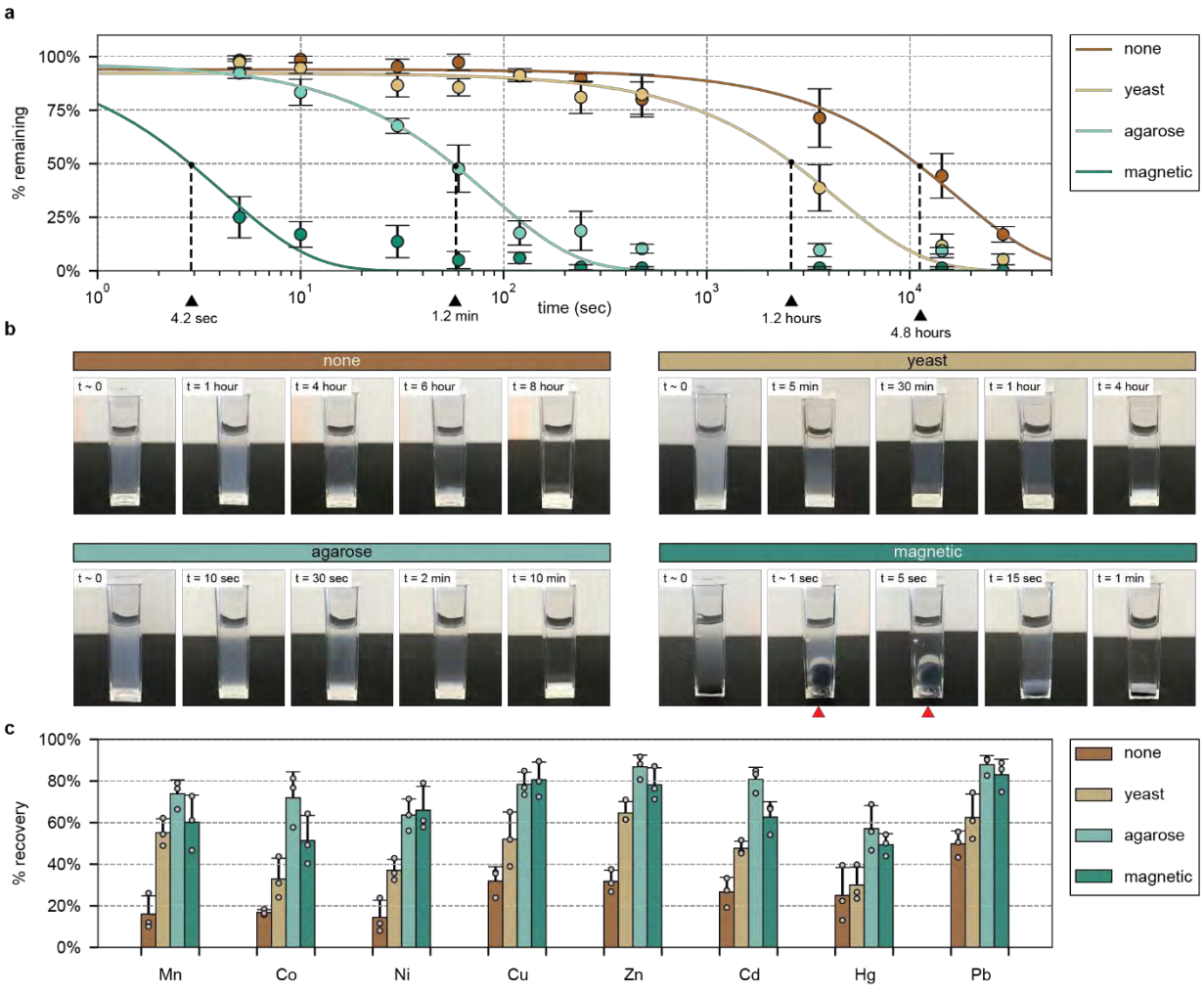


**Figure 5 | glnA fused with a 3XFlag tag, or using yeast displaying glnA monomers, improve sedimentation rates and metal recovery. a**) glnA+3XFlag was aggregated with 1 mM Cd and later mixed with anti-flag agarose or anti-flag magnetic beads, or glnA was mixed with yeast displaying glnA monomers. Magnetic beads had the quickest pull down of aggregates, followed by agarose beads, then yeast. **b**) Visual representation of aggregation sedimentation with yeast display, agarose, or magnetic beads. Red arrows for the magnetic beads indicate moments when an external magnet was used. **c**) Mixtures were allowed to sediment after 1 hour in which the sedimented pellet was isolated, washed, and extracted of metals using EDTA. Bars represent the percent metals recovered relative to the amount of metals removed by the protein aggregates. For all data, the mean ± s.d. of three replicates are shown.

| | | Mn | Co | Ni | Cu | Zn | Cd | Hg | Pb |
|---|---|---|---|---|---|---|---|---|---|
| pyrG | *A* | 0.1 ± 0.01 | 0.15 ± 0.07 | 0.20 ± 0.08 | 0.37 ± 0.04 | 0.20 ± 0.01 | 0.395 ± 0.05 | 0.243 ± 0.01 | 0.383 ± 0.01 |
| | $K_D$ | 0.5 ± 0.01 | 4.66 ± 0.43 | 3.7 ± 0.4 | 0.42 ± 0.2 | 0.57 ± 0.03 | 2.44 ± 0.12 | 0.13 ± 0.05 | 0.76 ± 0.04 |
| | *n* | 1.58 ± 0.21 | 12.43 ± 1.6 | 1.67 ± 0.87 | 11.06 ± 1.1 | 1.1 ± 0.06 | 0.66 ± 0.15 | 4.31 ± 1.96 | 1.59 ± 0.22 |
| glnA | *A* | 0.22 ± 0.01 | 0.15 ± 0.01 | 0.12 ± 0.01 | 0.21 ± 0.03 | 0.16 ± 0.002 | 0.18 ± 0.01 | 0.08 ± 0.01 | 1.37 ± 0.1 |
| | $K_D$ | 1.05 ± 0.02 | 0.48 ± 0.06 | 0.17 ± 0.01 | 0.61 ± 0.14 | 0.42 ± 0.05 | 0.8 ± 0.09 | 2.11 ± 0.86 | 2.18 ± 0.04 |
| | *n* | 32.86 ± 3.15 | 3.32 ± 1.76 | 4.57 ± 1.81 | 9.93 ± 1.3 | 3.25 ± 0.5 | 2.96 ± 0.76 | 1.33 ± 0.6 | 2.7 ± 0.14 |

**Table 1 | Values for maximum aggregation intensity (*A*; measured at 350 nm), aggregation $K_D$, and fitted cooperativity coefficient (*n*) for pyrG and glnA for the various metals studied.** Coefficients were fitted from data collected in Figure 2b.